Available online at www.sciencedirect.com
ScienceDirect
International Journal of Heat and Mass Transfer 50 (2007) 3019–3025
International Journal of HEAT and MASS TRANSFER
www.elsevier.com/locate/ijhmt

Local effects of longitudinal heat conduction in plate heat exchangers

Michele Ciofalo *

Dipartimento di Ingegneria Nucleare, Università degli Studi di Palermo, Viale delle Scienze, 90128 Palermo, Italy

Received 27 November 2006
Available online 1 March 2007

Abstract

In a plate heat exchanger, heat transfer from the hot to the cold fluid is a multi-dimensional conjugate problem, in which longitudinal heat conduction (LHC) along the dividing walls often plays some role and can not be neglected. *Large-scale*, or end-to-end, LHC is always detrimental to the exchanger's effectiveness. On the contrary, if significant non-uniformities exist in the distribution of either convective heat transfer coefficient, *small-scale*, or local, LHC may actually enhance the exchanger's performance by improving the thermal coupling between high heat transfer spots located on the opposite sides of the dividing wall.

Keywords: Longitudinal heat conduction; Conjugate heat transfer; Plate heat exchangers

1. Introduction

The elementary theory of heat exchangers [1] assumes that heat is transferred locally from the hot to the cold fluid through an interposed solid wall which only acts as a thermal resistance s/k, while conduction *along* the wall is neglected. The overall heat transfer coefficient is then

$$U = \left(\frac{1}{h_H} + \frac{s}{k} + \frac{1}{h_C}\right)^{-1} \quad (1)$$

with obvious modifications to account for fouling factors and geometrical effects.

In real equipment, however, heat transfer is actually a *multi-dimensional conjugate* problem, in which heat conduction not only in the direction orthogonal to the walls (*transverse* conduction), but also in that parallel to them (*longitudinal* conduction), may play a role.

The coupling between conduction through a solid wall and convection to a fluid is an issue in several classic problems of heat transfer, which are still actively studied. These include, for example, thermal entrance effects [2], fluid preheating [3], and heat transfer with a plate of finite thickness the outer surface of which is kept at a prescribed temperature [4].

In heat exchangers, it is important to separate the *large-scale* from the *small-scale* effects of longitudinal heat conduction (LHC).

Large-scale (end-to-end) LHC acts at the length scale of the whole unit, affects all kinds of heat exchangers, and is always detrimental to their thermal performance. Simplified models to estimate its effects have been presented, for example, by Shah [5] for recuperators and by Ranganayakulu et al. [6] for plate-fin and tube-fin exchangers. Chiou [7] proposed a quantitative criterion, based on the value of a "conductance number", to assess the relevance of LHC in compact heat exchangers. Large-scale LHC can become a very important issue in micro-channels and miniature heat transfer devices [8–10]. It can also be relevant in very high NTU exchangers such as the cryocoolers used in some space applications [11].

On the contrary, *small-scale* (local) LHC acts at the length scale of a unitary cell, depends on the existence of non-uniformities in the local convection coefficients, and is most significant in plate heat exchangers. The overall effects of conduction are implicitly taken into account by advanced, CFD-based, predictive techniques [12], but

* Tel.: +39 091 232 225; fax: +39 091 232 215.
E-mail address: ciofalo@din.din.unipa.it

0017-9310/$ - see front matter © 2007 Elsevier Ltd. All rights reserved.
doi:10.1016/j.ijheatmasstransfer.2006.12.006

Nomenclature

Bi_L, Bi_T	longitudinal and transverse Biot numbers, see text (–)
C	(flow rate) × (specific heat) (WK^{-1})
h	convection coefficient ($Wm^{-2}K^{-1}$)
h'	high value ("peak") of h in two-region approximation ($Wm^{-2}K^{-1}$)
h''	low value ("trough") of h in two-region approximation ($Wm^{-2}K^{-1}$)
k	thermal conductivity ($Wm^{-1}K^{-1}$)
L	unit cell length in flow direction (m)
R	resistance per unit depth (mKW^{-1})
S	heat transfer surface (m^2)
s	wall thickness (m)
T	temperature (K or °C)
U	overall heat transfer coefficient ($Wm^{-2}K^{-1}$)

Greek symbols

α, β, γ, η	dimensionless ratios, see text (–)
ε	exchanger effectiveness (–)
θ	temperature difference (K)

Subscripts

AV	average
C, H	cold-fluid/hot-fluid sides
L, T	longitudinal/transverse

simplified design procedures are still common and one would like to have approximate but viable methods to describe LHC effects by appropriate corrections to simpler correlations like Eq. (1).

2. Local effects of LHC in plate heat exchangers

Plate exchangers (PHX), though less common than the more traditional shell-and-tube exchangers, are widely used in the chemical, process and food industry [13]. In PHX, hot and cold fluids are separated by thin, usually metallic, plates; materials such as graphite, ceramics or even plastic may also be used for particular applications. Recently, PHX have been the subject of increasing interest due to the possibility of improving their performances, thus reducing volume and cost, by a relatively simple rational redesign of the basic heat transfer elements, based either on detailed local heat transfer measurements or on CFD.

A real PHX for industrial applications may include up to hundreds of tightly packed plates delimiting more or less tortuous flow passages. To optimize size, cost and effectiveness the overall exchanger may be divided into zones where either parallel flow or counter flow occurs. However, it is always possible to think of a real exchanger as composed of a very large number of *elementary cells* which repeat themselves periodically and usually exhibit a shape apt to promote mixing within each fluid and thus heat transfer between the two fluids.

In an elementary cell, the fluid-to-wall heat transfer coefficient h on each of the two sides of a plate exhibits a more or less complex distribution, associated with the existence of flow features such as separation, recirculation and reattachment. Detailed experimental results can be obtained, for example, by using liquid crystal thermography associated with true-colour digital image processing [14] and are usually well predicted by CFD methods [15].

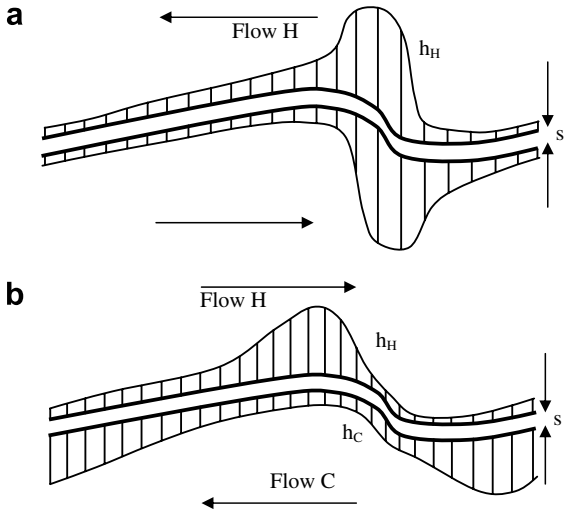

Fig. 1. Different distributions of the convective heat transfer coefficient h on the two sides of a plate in a PHX. (a) Matched h distributions; (b) unmatched h distributions. Plate geometry, h distribution and flow pattern are supposed to be periodic along the main flow direction.

For the sake of simplicity, Fig. 1 shows two possible h distributions for the simplified case of *two-dimensional* flow.

In some cases, see Fig. 1a, the distributions of h over the two sides may be approximately symmetric with respect to the dividing plate. In such cases, the plate only acts as an obstacle to heat transfer, and thus it is desirable that its transverse thermal resistance, proportional to s/k, be kept as low as possible compatibly with structural requirements. Standard formulae like Eq. (1) for the computation of the overall heat transfer coefficient U, once written using wall-averaged values of h on each side, will give fairly accurate results. This case is more likely to occur in parallel-flow regions and with only moderately tortuous flow passages.

In other cases, see Fig. 1b, the distribution of h over either of the two sides may match poorly that observed

on the opposite side of the dividing plate. This case is more likely to occur in counter-flow regions and in the presence of highly tortuous flow passages. In such cases, most of the thermal coupling between the two fluids may depend on the longitudinal conduction along the plate. As the wall thickness decreases, its longitudinal conductive thermal resistance increases; therefore, the thermal coupling between the two fluids decreases and the effective overall heat transfer coefficient U may become much lower than that predicted on the basis of mean values of each h. These coupling effects may affect heavily the overall performance of a PHX [16].

In the following, a simple model of the LHC effects will be described and its predictions will be compared with computational results obtained by CFD for geometrical and physical conditions representative of a PHX. It is formulated here for a two-dimensional geometry, but its extension to fully three-dimensional cases is relatively straightforward.

First, with reference to Fig. 2a, let us approximate the real (continuous) distribution of the convection coefficient h on either side of the dividing wall by a simple two-region stepped distribution, characterized by "peaks" and "troughs" of values h', h'' (with $\alpha = h'/h''$) and widths γL and $(1-\gamma)L$, respectively. Let also βL be the longitudinal distance between the hot and cold wall peak centres and $\eta = h''_C/h''_H$ (ratio of "trough" values of h).

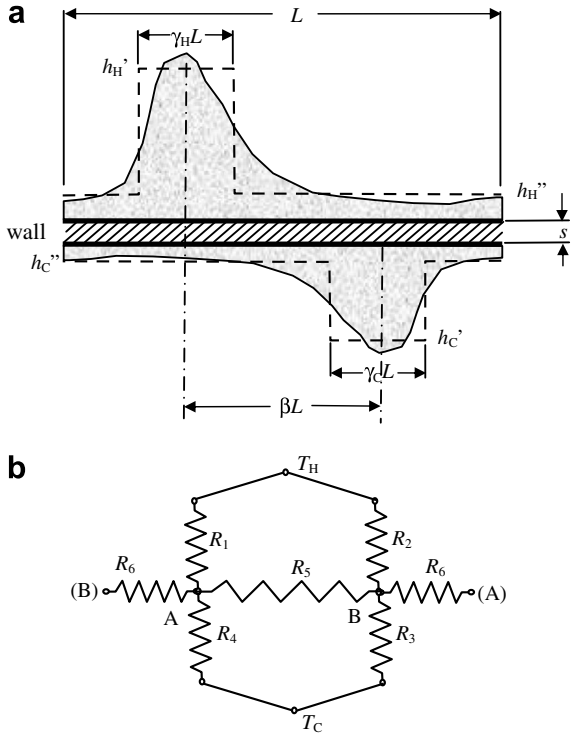

Fig. 2. (a) True profile (shaded area) and two-region approximation (broken line) of the convective heat transfer coefficient h distribution on the two sides of a plate in a PHX. (b) Equivalent resistance network.

Now, observe that the heat transfer process between the hot and cold fluids can be approximated as occurring through the resistance network of Fig. 2b. The equivalent thermal resistance network method has been commonly used to describe conjugate heat transfer problems [17]. It can be generalized by the inclusion of capacitors and nonlinear elements to simulate transient heat transfer and other particular thermal effects [18].

The quantities $R_1 \ldots R_6$ (thermal resistances per unit length in the direction orthogonal to the figure) in Fig. 2b have the following expressions:

$$R_1 = \frac{\alpha_H^{-1} + Bi_T}{L\gamma_H h''_H} \quad R_2 = \frac{1 + Bi_T}{L(1-\gamma_H)h''_H}$$
$$R_3 = \frac{(\eta\alpha_C)^{-1} + Bi_T}{L\gamma_C h''_H} \quad R_4 = \frac{\eta^{-1} + Bi_T}{L(1-\gamma_C)h''_H} \tag{2}$$
$$R_5 = \frac{\beta Bi_L}{Lh''_H} \quad R_6 = \frac{(1-\beta)Bi_L}{Lh''_H}$$

in which, besides the dimensionless ratios α_H, α_C, β_H, β_C, γ_H, γ_C and η defined above, the two following *Biot numbers* play a role:

$$Bi_T = \frac{sh''_H}{2k} \quad \text{(transverse Biot number)} \tag{3}$$

$$Bi_L = \frac{L^2 h''_H}{ks} \quad \text{(longitudinal Biot number)} \tag{4}$$

It should also be observed that the two resistances R_5, R_6 are actually *in parallel* due to the periodic geometry of the exchanger, so that they are equivalent to a single thermal resistance $R_L = \beta(1-\beta)Bi_L/(Lh''_H)$. Of course, the choice of h''_H as the reference heat transfer coefficient is arbitrary and any other h might have been used instead.

The (trivial, but cumbersome) resolution of the resistance network in Fig. 2b yields the following value for the overall heat transfer coefficient $U = (\text{power per unit area})/(T_H - T_C)$:

$$U = \frac{1}{L} \cdot \frac{(R_1+R_2)(R_3+R_4) + R_L(R_1+R_2+R_3+R_4)}{(R_2R_3R_4 + R_1R_3R_4 + R_1R_2R_4 + R_1R_2R_3) + R_L(R_1+R_4)(R_2+R_3)} \tag{5}$$

The above value can be compared with that predicted by Eq. (1) using average values of h_H and h_C. By using the dimensionless parameters defined above, this can be re-written as:

$$U_{avg} = h''_H \left[\frac{1}{1 + (\alpha_H - 1)\gamma_H} + 2Bi_T + \frac{\eta^{-1}}{1 + (\alpha_C - 1)\gamma_C} \right]^{-1} \tag{6}$$

Note that this value of U_{avg} cannot be obtained from Eq. (5) by letting $R_L \to 0$ due to the different assumptions underlying Eq. (5) and Eqs. (1) or (6). Note also that the ratio $F = U/U_{avg}$ depends only on dimensionless parameters and not on h''_H or L.

The influence of longitudinal heat conduction (LHC) is shown in Fig. 3 by reporting F as a function of Bi_T for different values of Bi_L, and in Fig. 4 by reporting F as a function of Bi_L for different values of Bi_T. In both figures it was assumed that $\alpha_H = \alpha_C = 3$, $\gamma_H = \gamma_C = 0.5$ and $\eta = 1$.

It can be observed that, for the highly non uniform h distributions assumed here, F decreases strongly with Bi_L (as expected) for all values of Bi_T. The influence of Bi_T is more complex; an increase in Bi_T causes F to decrease for strong longitudinal coupling, but to increase for the more likely case of loose longitudinal coupling (high Bi_L).

The use of the common design Eq. (1) – written on the basis of average h values, i.e. in the form of Eq. (6) – may lead to overpredicting the overall heat transfer coefficient U up to 25% for strongly non uniform h and high values of Bi_L.

In the limiting case of h distributions characterized on both sides of the wall by localized and unmatched peaks, with zero "trough" values, the overall heat transfer coefficient *vanishes* for high Bi_L, and only LHC effects provide for non-zero values of U.

An interesting effect of LHC is that, as the wall thickness s increases, the reduction in U due to a larger transverse

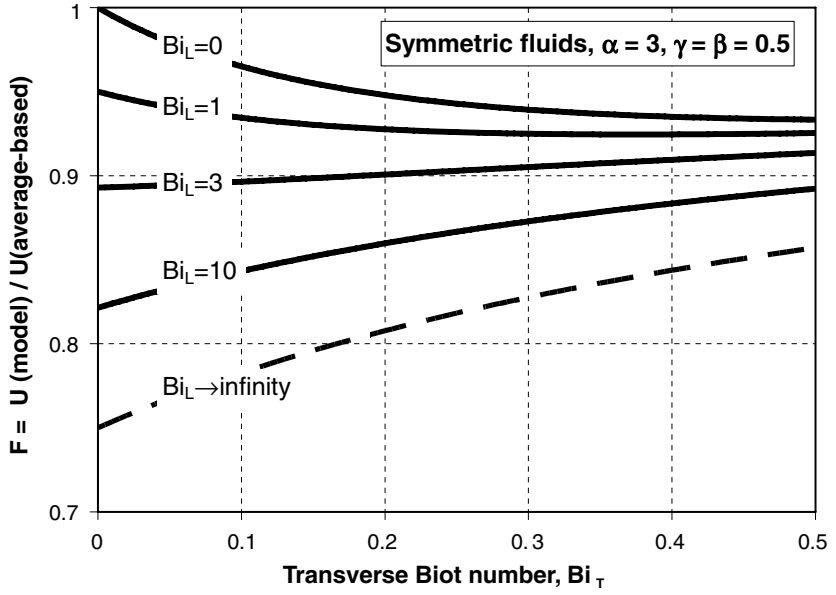

Fig. 3. Influence of LHC shown by expressing F as a function of Bi_T for different values of Bi_L.

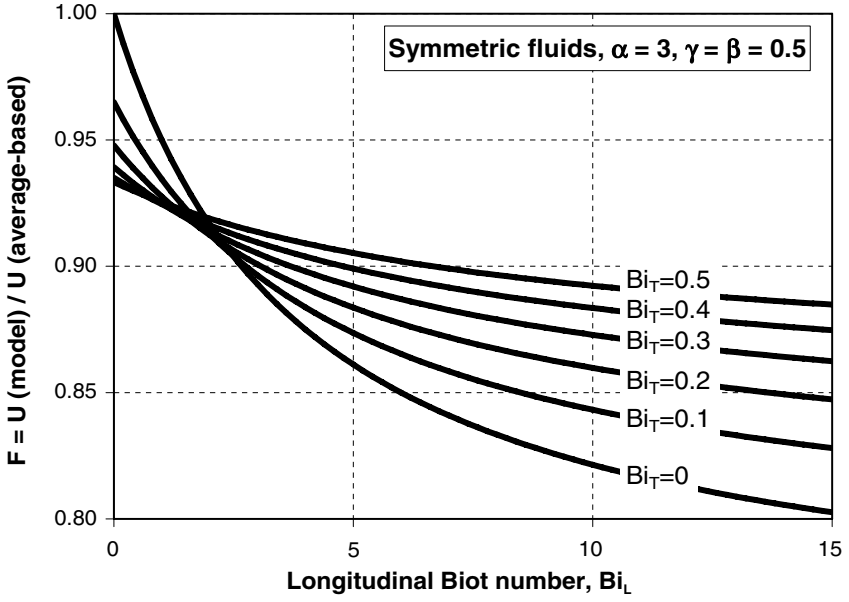

Fig. 4. Influence of LHC shown by expressing F as a function of Bi_L for different values of Bi_T.

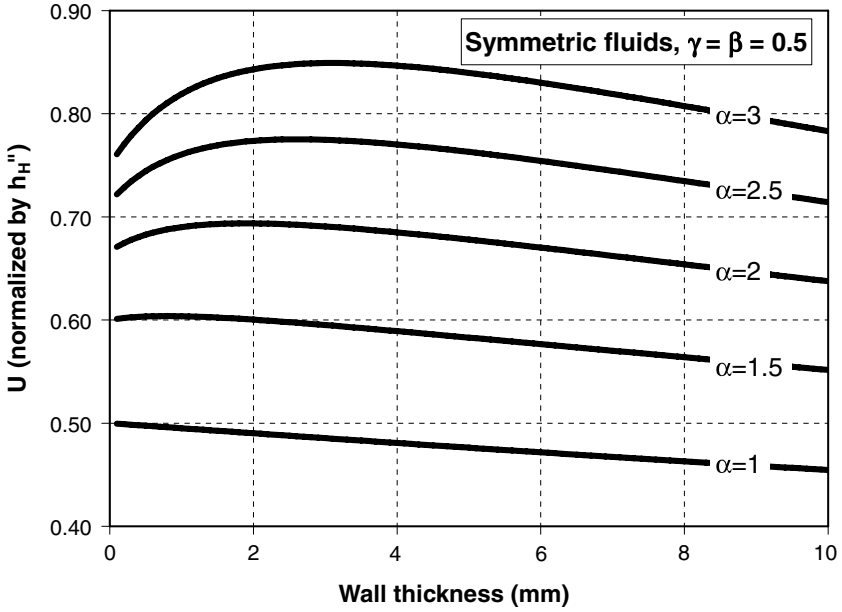

Fig. 5. Influence of the wall thickness s on the overall heat transfer coefficient U for different degrees of non-uniformity in the distributions of h.

conductive resistance may be counteracted by the increase in U due to a better longitudinal coupling, with the result that a maximum of U is attained for some value of s. This is illustrated in Fig. 5, which refers to the case of globally symmetric h distributions ($\alpha_H = \alpha_C = \alpha$, $\gamma_H = \gamma_C$, $\eta = 1$) with $\beta = 0.5$. The overall heat transfer coefficient U (normalized by h''_H) is reported as a function of the wall thickness s for different values of the h peaking factor α. Of course, the case of flat distributions of h ($\alpha = 1$) yields a monotonic decrease of U with s; however, for $\alpha > 1$ a maximum appears in the curves for values of s which increase with the degree of non uniformity.

The predictions provided by the LHC model described above were also tested against CFD results for two-dimensional conjugate heat transfer. The unitary cell of the geometry chosen is shown in Fig. 6; it is representative of a plate heat exchanger in which plane plates are alternately stacked with sinusoid-shaped plates. The RNG k–ε turbulence model was adopted to simulate the flow of water on either side of the plate at a Reynolds number of ~3000. The simulations were run by using the computer code CFX-4.3 [19]. Note that, although computational results can not generally be regarded as completely trustworthy (especially when turbulent flow is involved), in the present case they can be considered sufficiently accurate to test an explicitly crude model such as the resistance network one.

Fig. 7 shows the computed profiles of the convective heat transfer coefficient on the two sides of the plate for either parallel flow or counter flow. It can be observed that the h distributions are identical but are shifted by half pitch and, in the case of counter flow, also mirror-reflected.

The h distributions in Fig. 7 were approximated by using the two-region model with $\alpha = 2$, $\gamma = 0.5$ on both sides and

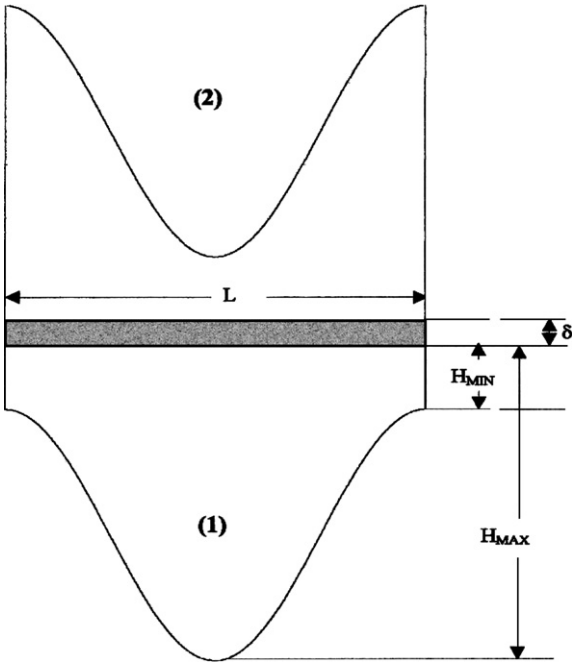

Fig. 6. Geometry chosen for the CFD conjugate heat transfer simulations.

$\eta = 1$, $\beta = 0.5$. In the CFD simulations, the transverse and longitudinal Biot numbers Bi_T, Bi_L were independently allowed to vary by assuming two different thermal conductivities k_T, k_L of the plate in the two mutually orthogonal directions.

Results are summarized in Fig. 8 for two rather extreme values of Bi_T (0.0066 and 0.66) and for Bi_L varying from ~0.6 to ~250. The quantity shown is the ratio of U to that given by Eq. (6). The agreement is quite satisfactory, indicating that the simple network-of-resistances model is

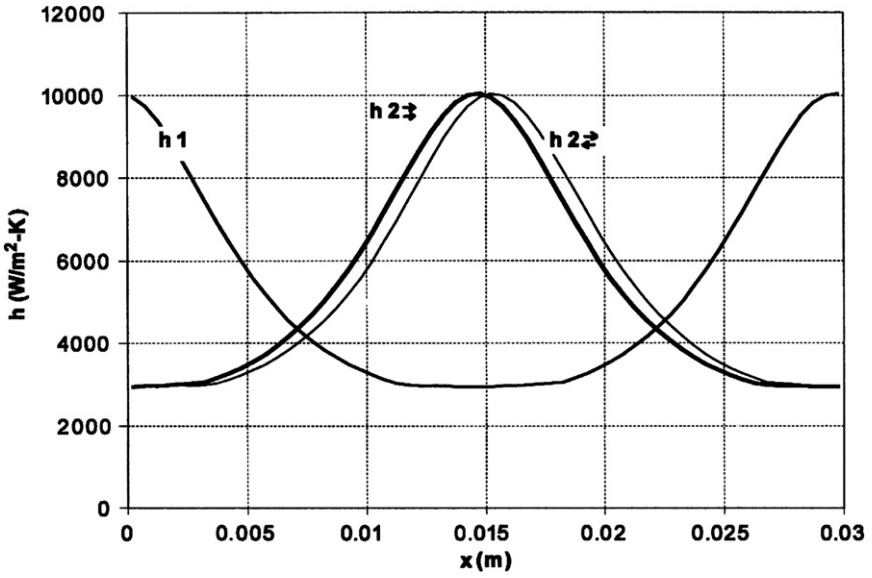

Fig. 7. Computed profiles of the convective heat transfer coefficient h on the two sides. Profiles of h_2 are reported both for the case of parallel flow and for the case of counter flow.

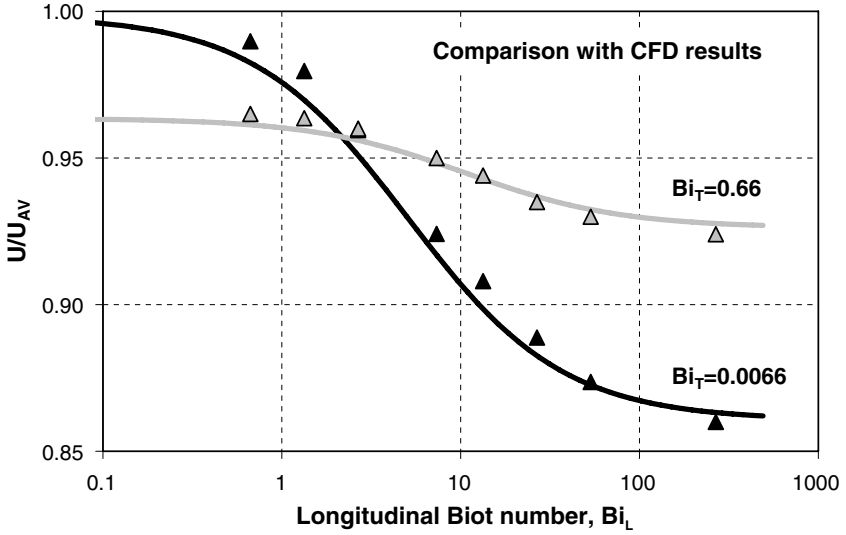

Fig. 8. Comparison of predictions obtained by the network-of-resistances model (lines) and by computational fluid dynamics (symbols).

adequate to capture most of the significant features of LHC-associated phenomena.

3. Conclusions

The influence of longitudinal heat conduction (LHC) on heat exchanger performance was briefly reviewed. Large-scale and small scale LHC were separately treated as they may have contrasting effects on heat transfer. For small-scale effects, related with non-uniform and unmatched distributions of the convection coefficient h and most significant in plate heat exchangers, a simplified model was presented, based on the concept of network of resistances (NOR), and its predictions were discussed. In particular, it was shown that LHC may significantly enhance heat transfer and may cause the overall heat transfer coefficient U to exhibit a maximum when represented as a function of the wall thickness s. The results provided by the simple NOR model compared favorably with CFD predictions, in which convection in the fluids and conduction in the wall were simultaneously taken into account.

The simple model proposed here can be used to get a quick and inexpensive estimate of the actual overall heat transfer coefficient U for *any* thickness s and conductivity k of the interposed plate once the distribution of the convective heat transfer coefficient h on the two sides is known,

for example from a single CFD analysis (making, of course, the reasonable assumption that h itself is flow-dominated and little affected by conduction phenomena).

References

[1] F.P. Incropera, D.P. De Witt, Introduction to Heat Transfer, third ed., John Wiley & Sons, New York, 1996.

[2] Ş Bilir, A. Ateş, Transient conjugated heat transfer in thick walled pipes with convective boundary conditions, Int. J. Heat Mass Transfer 46 (2003) 2701–2709.

[3] S. Piva, Axial wall conduction preheating effects in high Péclet number laminar forced convection, Int. J. Heat Mass Transfer 39 (1996) 3511–3517.

[4] K. Chida, Surface temperature of a flat plate of finite thickness under conjugate laminar forced convection heat transfer condition, Int. J. Heat Mass Transfer 43 (2000) 639–642.

[5] R.K. Shah, A review of longitudinal wall heat conduction in recuperators, J. Energy Heat Mass Transfer 16 (1994) 15–25.

[6] Ch. Ranganayakulu, K.N. Seetharamu, K.V. Sreevatsan, The effects of longitudinal heat conduction in compact plate-fin and tube-fin heat exchangers using a finite element method, Int. J. Heat Mass Transfer 40 (1997) 1261–1277.

[7] J.P. Chiou, The advancement of compact heat exchanger theory considering the effects of longitudinal heat conduction and flow nonuniformity, in: R.K. Shah, C.F. Mcdonald, C.P. Howard (Eds.), Symposium on Compact Heat Exchangers, HTD, vol. 10, ASME, New York, 1980, pp. 101–121.

[8] I. Tiselj, G. Hetsroni, B. Mavko, A. Mosyak, E. Pogrebnyak, Z. Segal, Effect of axial conduction on the heat transfer in micro-channels, Int. J. Heat Mass Transfer 47 (2004) 2551–2565.

[9] Z.-Y. Guo, Z.-X. Li, Size effect on single-phase channel flow and heat transfer at microscale, Int. J. Heat Fluid Flow 24 (2003) 284–298.

[10] G. Maranzana, I. Perry, D. Maillet, Mini- and micro-channels: influence of axial conduction in the walls, Int. J. Heat Mass Transfer 47 (2004) 3993–4004.

[11] S.P. Narayanan, G. Venkatarathnam, Performance degradation due to longitudinal heat conduction in very high NTU counterflow heat exchangers, Cryogenics 38 (1998) 927–930.

[12] M. Ciofalo, I. Di Piazza, A computational approach to conjugate heat transfer between two fluids in plate heat exchangers of arbitrary geometry, Int. J. Heat Exchangers 3 (2002) 1–32.

[13] R.K. Shah, Heat Exchangers, in: A. Bisio, S. Boots (Eds.), Encyclopedia of Energy Technology and the Environment, John Wiley & Sons, New York, 1995, pp. 1651–1670.

[14] J.A. Stasiek, M.W. Collins, M. Ciofalo, P.E. Chew, Investigation of flow and heat transfer in corrugated passages – I. Experimental results, Int. J. Heat Mass Transfer 39 (1996) 149–164.

[15] M. Ciofalo, M.W. Collins, J.A. Stasiek, Investigation of flow and heat transfer in corrugated passages – II. Numerical simulations, Int. J. Heat Mass Transfer 39 (1996) 165–192.

[16] M. Ciofalo, Conjugate heat transfer in plate heat exchangers, in: Proceedings of the Third International Conference on Heat Powered Cycles – HPC 2004, Larnaca, Cyprus, 11–13 October 2004.

[17] S.H. Chong, K.T. Ooi, T.N. Wong, Optimisation of single and double layer counter flow microchannel heat sinks, Appl. Therm. Eng. 22 (2002) 1569–1585.

[18] J. Zueco, F. Alhamab, C.F. González Fernández, Analysis of laminar forced convection with network simulation in thermal entrance region of ducts, Int. J. Therm. Sci. 43 (2004) 443–451.

[19] AEA Technology, CFX release 4.3 – User guide, AEA Report, Harwell, UK, 2000.